Received: 1 December 2018 | Revised: 6 December 2019 | Accepted: 8 January 2020

DOI: 10.4218/etrij.2018-0632

ORIGINAL ARTICLE

ETRI Journal WILEY

Energy-efficient data transmission technique for wireless sensor networks based on DSC and virtual MIMO

Manish Kumar Singh[1,2] | Syed Intekhab Amin[2]

[1]KIET Group of Institutions, Ghaziabad, India

[2]Jamia Millia Islamia, New Delhi, India

Correspondence
Manish Kumar Singh, KIET Group of Institutions, Ghaziabad, India.
Email: mks.manish1983@gmail.com

In a wireless sensor network (WSN), the data transmission technique based on the cooperative multiple-input multiple-output (CMIMO) scheme reduces the energy consumption of sensor nodes quite effectively by utilizing the space-time block coding scheme. However, in networks with high node density, the scheme is ineffective due to the high degree of correlated data. Therefore, to enhance the energy efficiency in high node density WSNs, we implemented the distributed source coding (DSC) with the virtual multiple-input multiple-output (MIMO) data transmission technique in the WSNs. The DSC-MIMO first compresses redundant source data using the DSC and then sends it to a virtual MIMO link. The results reveal that, in the DSC-MIMO scheme, energy consumption is lower than that in the CMIMO technique; it is also lower in the DSC single-input single-output (SISO) scheme, compared to that in the SISO technique at various code rates, compression rates, and training overhead factors. The results also indicate that the energy consumption per bit is directly proportional to the velocity and training overhead factor in all the energy saving schemes.

KEYWORDS
cluster head, CMIMO, distributed source coding, DSC-MIMO, sensor nodes, wireless sensor network

1 | INTRODUCTION

The total energy consumption in any communication system consists of transmission and circuit energy consumption. The transmission energy consumption exceeds the circuit energy consumption in total energy consumption in long-distance communication. However, in short-distance communication, circuit energy consumption is higher than the transmission energy consumption. Therefore, energy-efficient wireless sensor network (WSN) schemes focus on reducing both the transmission and circuit energy consumption [1]. The multiple-input multiple-output (MIMO) scheme is an effective scheme for reducing energy consumption in the WSN. However, in WSNs, the physical size of the sensor nodes is limited, and therefore, installing multiple antennas at the sensor nodes is not ideal. Thus, cooperative MIMO (CMIMO) can be achieved by orchestrating collaboration among the single antennas installed on each sensor node. Therefore, spatial multiplexing can enhance the data rates, whereas spatial diversity can improve the bit-error rate (BER) by using the CMIMO technique [2,3]. However, a MIMO system has a higher circuit complexity that requires more circuit energy than a single-input single-output (SISO) system. Therefore, the MIMO scheme is suitable only for long-range communication, whereas the SISO scheme is suitable for short-range communication [3]. Thus, to achieve a long transmission range, more cooperative sensor nodes should be utilized to reduce the transmission energy via antenna diversity, and for the short transmission range, fewer cooperative nodes are chosen for reducing the circuit energy consumption [4].

In the CMIMO scheme, nodes cooperate to design clusters, providing maximum coverage region and minimum energy consumption with relatively uniform distribution of load within the networks. Densely deployed WSNs are generally dispersed over large areas and have a mesh topology structure. The sensor nodes are designed to power on and off in various modes, to reduce their energy consumption. In the WSNs, clustering requires grouping the sensor nodes, and selecting a cluster head (CH). Within the cluster, the sensor nodes send their data directly to the CH. The CHs then forward the total data to the sink (base station) directly or via multihops communication using other CHs as intermediate forwarding sensor nodes [5]. In a wide-ranging WSN, the energy consumption of the nodes is directly proportional to the transmission range. If some of the nodes deplete their energy too early, they will seriously reduce the reliability of the WSN. To enhance the reliability of the WSN, the node density must be increased. However, correlated information collected from the neighboring nodes are directly proportional to sensor node density. These correlated data are transmitted to a base station (BS), as a result of which energy efficiency of the WSNs to decreases [6,7]. A virtual MIMO has a similar effect as a MIMO system in the WSNs; it reduces the energy consumption of the WSNs and resolves the energy consumption problem of the entire network [8]. However; a virtual MIMO cannot fix the low energy-efficiency condition in the entire high-density WSN that occurs as a result of a highly correlated source data. To resolve this issue, the distributed source coding (DSC) scheme based on the CMIMO scheme can be used [9,10]. Data aggregation and DSC are two different techniques for data collection. The former utilizes joint encoding, but separate decoding of the information, whereas, the latter utilizes separate data encoding and joint decoding. This important feature of DSC scheme is utilized for multi-rate data transmission in WSNs [7]. Binary phase-shift keying (BPSK) is a proven energy-efficient modulation technique for virtual MIMO data transmission scheme.

In [1], Cui and others proved that in long-range sensor networks, total delay and total consumption of energy can be minimized by using the CMIMO technique, rather than the SISO scheme. In [2] and [8], the authors revealed that even with the extra training overhead required in the CMIMO scheme, communication based on it can conserve sufficient energy in long-distance communication, in contrast to the SISO scheme. In the WSN, the selection of clusters and cluster heads is based on factors such as the residual energy of a node, geographic location, and link quality [5]. In [9], Abughalieh and others demonstrated that the lifetime of a WSN can be improved through compression of the correlated information, using the DSC scheme. In [6] and [10], the authors proved that the DSC-MIMO technique reduces energy consumption through the MIMO scheme, and enhances energy efficiency by compressing the correlated data using the DSC scheme. Sartipi and others [11,12] revealed that the DSC of two correlated source nodes at any arbitrary rate is based on the Slepian-Wolf (SW) theorem. In [13], the authors demonstrated that applications based on medical imaging and video systems, contain large amounts of data to be transmitted, and thus, the radio transceiver sensor nodes drain more energy than the receiver sensor nodes.

To clarify the importance of our work, we will discuss the benefits of the DSC-MIMO, compared to the CMIMO or DSC schemes used alone in the WSN. The CMIMO reduces the energy consumption in the WSN, whereas the DSC compresses the correlated communication data in sensor nodes and enhances the energy efficiency of the WSN. First, we perform the mathematical modeling of SISO, MIMO, DSC-SISO, and DSC-MIMO; then, we compare their total energy consumption over selected transmission distances for the same BER. This study is quite different from previous studies, because we show the effect of SISO, MIMO, DSC-SISO, and DSC-MIMO on the total energy consumption for various code rates and compression rates, in addition to considering the training overhead factor. Data compression in the DSC-MIMO is based on the SW theorem. The conditions for the boundary value of velocity and training overhead factor are also proposed as better guidelines. In the WSN, the training overhead and velocity have respective critical values, beyond which the WSN will not be realistic. This paper also discusses the effect of velocity on total energy consumption.

The rest of the paper is organized as follows. In Section 2, data compression using the DSC is presented. The DSC-MIMO is discussed in Section 3. Sections 4, 5, and 6 depict the energy consumption model and its analysis. Finally, the paper is concluded in Section 7.

2 | DATA COMPRESSION USING DSC

2.1 | Types of data compression

There are two types of data compression, lossless and lossy compression, based on whether, or not, following data compression, all original information can be recovered as the data are uncompressed.

In the lossless compression, every information bit that was initially in the data is retained, after the data are compressed. All the data are fully restored following decompression. In this operation, no information is lost. In contrast, in lossy compression, some data, mainly redundant data, are compressed. Thus, some information is lost following data compression.

2.2 | Source coding theorem

If a random variable X represents the output of a discrete memoryless source, then for any source coding technique, the entropy of X sets the following conditions for the average codeword length, "L":

$$L \geq H(X). \tag{1}$$

According to this theorem, the average codeword length for any coding scheme can be reduced, as long as it is not less than entropy $H(X)$; thus,

$$L_{\min} = H(X) \tag{2}$$

where $L_{\min}$ represents minimum value of L.

The entropy of the sources sets up the fundamental limit on the elimination of redundancy from the information [14,15].

2.3 | Distributed source coding

The DSC is utilized if there is a correlation between the nodes. This is precisely the case in the conventional WSNs, where correlation is generally quite high between adjacent nodes [9]. To exploit this correlation, and eliminate redundancy, every sensor node knows about the information being sent by different sensor nodes. This can be realized in two ways: either the sensor nodes can exchange the information with each other, or they could be prevented from utilizing this scheme. The primary alternative exerts an additional undesirable overburden on the sensor network and demands extra processing of information in every node. The purpose of the DSC in the sensor network is completely the inverse of the first technique. Therefore, the second technique is chosen to minimize the amount of processing, and, by extension, the energy consumption [10]. The concept of the DSC is based on the SW coding theorem. Accordingly, the effective compression of, at least two sources can be accomplished by separate encoding and combined decoding [16–18].

According to the SW theorem, data compression can be performed in a completely blind manner in the WSN. The implication of this is that the sensor nodes only have knowledge of local data, that is, they compress the information without knowledge of the information in the other sensor nodes. Hence, the sensor nodes do not communicate among themselves during data compression. Therefore, the DSC is a key technique for compressing the data and improving the energy efficiency of the WSNs [11,12,19]. If X is an information source, then information rate, $R \geq H(X)$, is necessary to transmit source X to the sink (base station), where $H(X)$ is the entropy of any random source, X. Figure 1 shows the SW coding for two correlated sources. In Figure 1, X_1 and X_2 are two independent random correlated sources that are encoded separately and decoded jointly. According to the SW theorem for correlated sources:

$$\text{Total rate } R = R_{X1} + R_{X2} \tag{3}$$

and

$$R_{X1} + R_{X2} \geq H(X_1) + H(X_2) \tag{4}$$

where R_{X1} and R_{X2} are the compression rates and $H(X_1)$ and $H(X_2)$ are the entropies of sources X_1 and X_2. Figure 2 shows the rate region for the SW coding. According to the SW coding theorem, the achievable rate region is determined by the following equations:

$$R_{X1} \geq H\left(\frac{X_1}{X_2}\right), \tag{5}$$

$$R_{X2} \geq H\left(\frac{X_2}{X_1}\right), \tag{6}$$

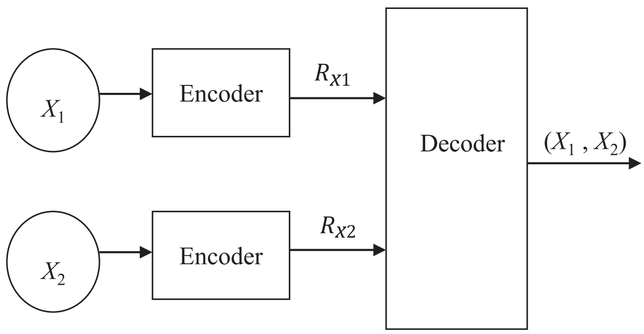

FIGURE 1 SW coding for two correlated sources

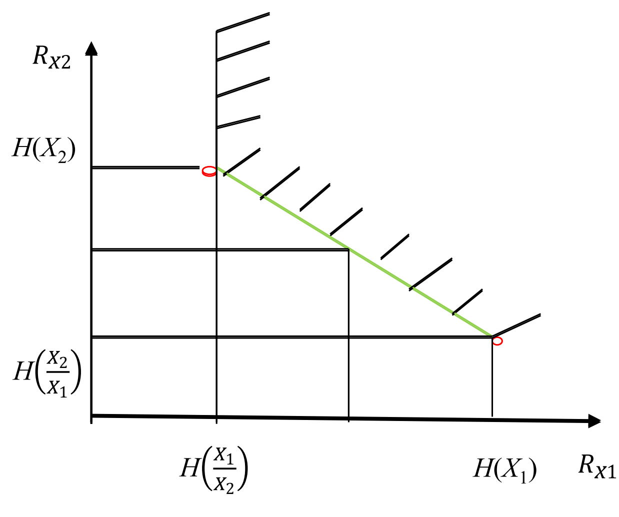

FIGURE 2 SW coding (rate region)

$$R_{X1}+R_{X2}\geq H\left(X_1,X_2\right). \tag{7}$$

In Figure 2, the green line denotes the minimum theoretical rate for two correlated sources, and the red dots at the corners represent the optimum rate region, similar to the following rates:

$$R_{X1}=H\left(X_1\right) \text{ and } R_{X2}=H\left(\frac{X_2}{X_1}\right)\text{, or}$$

$$R_{X1}=H\left(\frac{X_1}{X_2}\right)\text{, and } R_{X2}=H\left(X_2\right). \tag{8}$$

In Figure 3, X_1 and X_2 are two source nodes. The nearest node (X_1) to the sink (base station) has to perform encoding at a rate equal to its entropy, and the second nearest node (X_2) to the sink (base station) has to perform encoding at a rate equal to the conditional entropy of itself and the first source available at the base station, and so on. The sensor node X_1 transmits uncompressed data to the decoder, as shown in Figure 3. Node X_2 is the input of the encoder that compresses the data of Node X_2, that is, it underscores the correlation between sensor nodes X_1 and X_2. The more the data correlation between the source nodes, that is, X_1 and X_2, the more compressed the data of sensor node X_2.

Similarly, in Figure 4, if X_1, X_2, X_3, …, X_N are N different source nodes that, transmit data to the sink node, and their encoding rates are R_1, R_2, R_3, …, R_N, then, according to the SW encoding, we obtain the following:

$$R_1\geq H\left(X_1\right), \tag{9}$$

$$R_2\geq H\left(\frac{X_2}{X_1}\right), \tag{10}$$

$$R_3\geq H\left(\frac{X_3}{X_1},X_2\right), \tag{11}$$

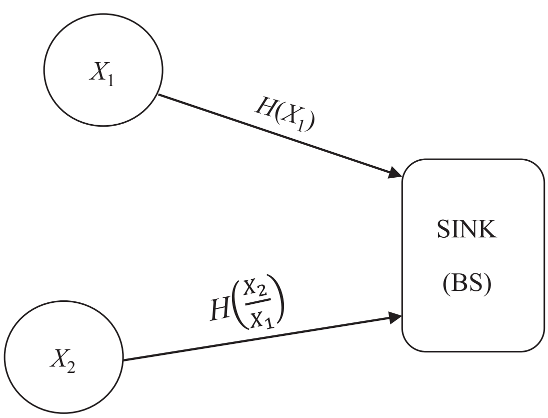

FIGURE 3 Two source nodes for WSN

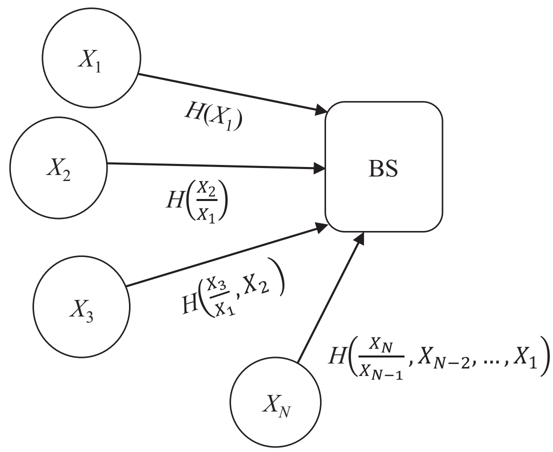

FIGURE 4 N source nodes for WSN

$$R_N\geq H\left(\frac{X_N}{X_{N-1}},X_{N-2},\ \dots,X_1\right). \tag{12}$$

Let R_{X_a} be the compression rate of Source X_a, then the SW rate for the DSC of N sources is.

$$R_{Xa1}+R_{Xa2}+\ldots+R_{Xal}\geq H(X_{a1},...,X_{al}/X_{b1},...,X_{bN-l}) \tag{13}$$

where $l\leq N$, $(a_1, a_2, \dots, a_l)\subseteq(1, \dots, N)$ and $(b_1, b_2, \dots, b_{N-l}) = \{1,\ \dots,N\}/\left\{a_1,a_2,\ \dots,a_l\right\}$.

3 | DSC –MIMO

The DSC-MIMO is dependent on the cooperative groups (CGs), all of which are composed of two correlative source sensor nodes. The DSC first compresses the correlated source data, then, transmits the compressed information directly over a MIMO link to the next hop receiver, without transferring it to the CH, thus lessening the time taken to transfer the source data, and boosting the energy efficiency. Finally, we can utilize this new scheme, that is, DSC-MIMO, to save power and bandwidth, and enhance the energy efficiency of the WSNs. We can implement any of the DSC methods, such as turbo code, low density parity check (LDPC) code, and raptor code, with the CMIMO technique as needed. In this study, the LDPC code-based virtual MIMO is used, because it has several advantages over turbo and other codes. First, low-complexity decoders are used in LDPC codes. Secondly, every decoder decodes its information separately. If a fault occurs in a decoder, other decoders are not affected by the error. One practical problem in LDPC codes is that their encoding complexity is high. Two source nodes in a CG, X_1 and X_2, transmit k bits of source data in Figure 5. In the encoding process, X_1 is fed at a rate, R_1, into an LDPC

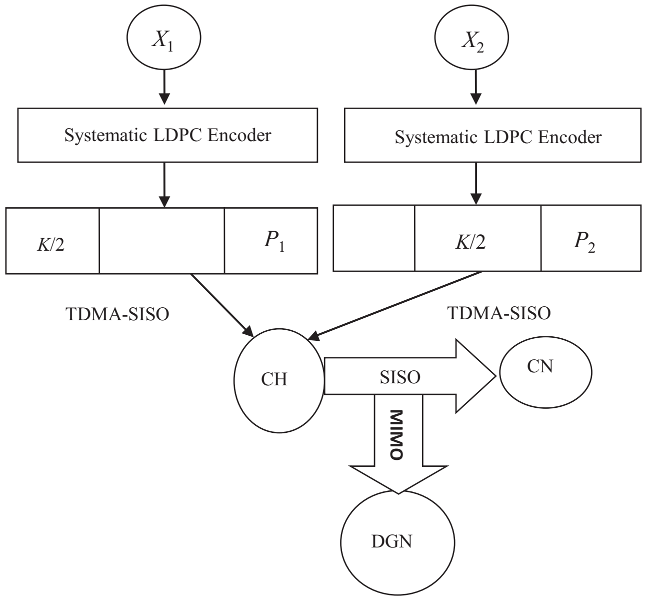

FIGURE 5 DSC-MIMO transmission procedure

encoder. At the encoder output, it transmits the parity bit P_1 and the first half of the information bits. Therefore, the source encoding rate is $R_{X1} = \{(k/2)+P_1\}/k$ bit-per-input-bit, and that imposes a rate of systematic LDPC code, $(R_1) = 1/\{R_{X1} + (1/2)\}$. The compression processes of the source nodes, X_2, and X_1 are similar; the only difference being that source node X_2 transmits the second half of the information bit and its related parity bit, P_2. The compression rates of both source nodes are identical, and that of related LDPC codes is equal [6,12].

Therefore, it is required to design a single systematic LDPC code to compress the two correlated sources with the DSC at a symmetric rate. At the receiver, the decoders recover both sources, X_1 and X_2. The CH and cluster node (CN) design a virtual multi-antenna array and send the information to the sink (DGN) through a virtual MIMO link. Once clustering is finished, the DSC-MIMO begins to form the routing table in the entire WSN. The DSC-MIMO uses the Dijkstra algorithm to build a routing table that is analogous to the CMIMO in the WSN. The Dijkstra algorithm provides the shortest routing path for every cluster. The LDPC codes are better than the block and convolution codes and can compete favorably with the turbo codes. Recent research works have proven that the LDPC codes are very desirable for WSNs, because of their applications in DSC and data compression [20].

4 | ANALYSIS OF ENERGY CONSUMPTION OF DSC-MIMO

Generally, in the WSN, the total power consumption includes two parts: the power consumption in all the amplifiers (P_{PA}), and the power consumption in other circuit blocks (P_{c}).

$$P_{\mathrm{PA}}(d) = (1+\alpha)\, P_{\mathrm{out}}(d) \tag{14}$$

where α is related to drain efficiency

$$P_{\mathrm{out}}(d) = \overline{E}_{\mathrm{b}} R_{\mathrm{b}} \frac{(4\pi)^2 d^{\beta} M_1 N_f}{G_{\mathrm{t}} G_{\mathrm{r}} \lambda^2} \tag{15}$$

where R_{b} denotes the bit rate, G_{t} denotes the transmitter antenna gain, and G_{r} denotes the receiver antenna gain, λ denotes the carrier wavelength, d denotes the transmitting distances, M_1 denotes the link margin, β denotes the path-loss exponent, N_{o} denotes the power spectral density, E_{b} denotes the energy per bit for a given BER that can be determined by the following equation:

$$\begin{aligned}\overline{P}_{\mathrm{b}} = \frac{4}{b}\left(1-\frac{1}{2^{b/2}}\right)\frac{1}{2^{N_{\mathrm{T}}N_{\mathrm{R}}}}\left(1-\frac{1}{\sqrt{1+2N_{\mathrm{o}}/E_{\mathrm{b}}}}\right)^{N_{\mathrm{T}}N_{\mathrm{R}}} \times \\ \sum_{k=0}^{N_{\mathrm{T}}N_{\mathrm{R}}-1}\frac{1}{2^{\beta}}\begin{pmatrix} N_{\mathrm{T}}N_{\mathrm{R}}-1+\beta \\ \beta \end{pmatrix}\times\left(1+\frac{1}{\sqrt{1+2N_{\mathrm{o}}/E_{\mathrm{b}}}}\right)^{\beta}\end{aligned} \tag{16}$$

where $\overline{P}_{\mathrm{b}}$ denotes the BER, N_{T} denotes the number of the sender nodes, N_{R} denotes the number of the receiver nodes, and b denotes the constellation size. Thus,

$$\begin{aligned}P_C = N_{\mathrm{T}}\left(P_{\mathrm{mix}} + P_{\mathrm{DAC}} + P_{\mathrm{filt}}\right) + 2P_{\mathrm{synth}} \\ + N_{\mathrm{R}}\left(P_{\mathrm{mix}} + P_{\mathrm{LNA}} + P_{\mathrm{IFA}} + P_{\mathrm{filr}} + P_{\mathrm{ADC}}\right)\end{aligned} \tag{17}$$

where P_{DAC} and P_{ADC} denote the power consumed by the digital-to-analog and analog-to-digital converter, P_{filt} and P_{filr} denote the power consumed by the filter at the transmitter's end and receiver's end; P_{mix}, P_{synth}, P_{IFA}, and P_{LNA} denote the power consumed by the mixer, frequency synthesizer, intermediate frequency amplifier, and low-noise amplifier, respectively.

Now, the total energy consumption per bit is as follows:

$$E_{\mathrm{pb}} = \frac{P_{\mathrm{PA}} + P_{\mathrm{c}}}{R_{\mathrm{b}}.}. \tag{18}$$

R_{b} can be changed by $R_{\mathrm{b}}^{\mathrm{eff}} = R_{\mathrm{b}}\frac{(F-pN_{\mathrm{T}})}{F}$. where pN_{T} training symbols are introduced in every block. F is the block size that is equal to $T_{\mathrm{C}}R_{\mathrm{S}}$; T_{C} represents the fading coherence time; and R_{S} represents the symbol rate. The coherence time $T_{\mathrm{C}} = 3/4f_m\sqrt{\pi}$; the maximum Doppler shift, $(f_m) = v/\lambda$, where v denotes the velocity [21]. The total energy consumption per bit when pN_{T} training symbols are introduced in every block is as follows:

$$E_{\mathrm{pbt}} = \frac{F}{(F-pN_T)}\left[\frac{P_{\mathrm{PA}} + P_{\mathrm{c}}}{R_{\mathrm{b}}}\right] \tag{19}$$

where p denotes the training overhead factor. In the intra-cluster communication, after the DSC, the sensor nodes that belong to a CG exchange their information using the SISO scheme. Then, the energy consumption per bit is

$$E_{\mathrm{pbt}}^{\mathrm{DSC-SISO}}(d) = \frac{F}{(F - pN_{\mathrm{T}})}\left[E_{\mathrm{pb}}(d)\,|_{N_{\mathrm{T}}=1, N_{\mathrm{R}}=1}\right] R_{X1} \tag{20}$$

where R_{X1} is the compression rate of the DSC.

In the intercluster communication, all the CGs communicate with the next master CG through a 2×2 virtual MIMO link. Therefore, the energy consumption per bit is

$$E_{\mathrm{pbt}}^{\mathrm{DSC-MIMO}}(d) = \frac{F}{(F - pN_{\mathrm{T}})}\left[E_{\mathrm{pb}}(d)\,|_{N_{\mathrm{T}}=2, N_{\mathrm{R}}=2}\right] R_{X1}. \tag{21}$$

There are G CGs, and after the space-time coding, each source node has L-bit data in intercluster communication. The total energy consumed by the DSC-MIMO in the intercluster communication process is as follows:

$$E_{\mathrm{inter}}^{\mathrm{DSC-MIMO}} = 2GLE_{\mathrm{pbt}}^{\mathrm{DSC-MIMO}}. \tag{22}$$

4.1 | Code rate (R_1) and compression rate (R_{X1})

$$\text{Data Compression rate }(\%) = \frac{\text{Total length of data after compression}}{\text{Total length of data before compression}} \times 100. \tag{23}$$

For a code whose block length (n-bits codewords) has k information bits and r parity bits, the code rate (R_1) is defined as the ratio of information bit to block length.

$$\text{Code rate }(R_1) = \frac{\text{Information bits }(k)}{\text{Block length }(n)}. \tag{24}$$

The code rate measures the redundancy in the block code [22].

The compression rate of source X_1 is

$$R_{X1} = \frac{(k/a) + P_1}{k}. \tag{25}$$

Then, the code rate $(R_1) = \frac{k}{k+P_1} = \frac{1}{R_{X1}+(1-1/a)}$

$$\text{If } a = 2, \text{ then, } \quad R_1 = \frac{1}{R_{X1} + 1/2}. \tag{26}$$

The same process is applied to source node X_2. The source encoder transmits the remaining information bit, as well as the related parity bit. The compression rate of the source node, X_2 is given as $R_{X2} = \{(a-1/a)k + P_2\}/k$.

The LDPC code rate of source X2 is:

$$R_2 = \frac{1}{R_{X2} + 1/a} = \frac{1}{R_{X2} + 1/2}. \tag{27}$$

5 | SIMULATION ANALYSIS

We utilized the MATLAB tool for simulation. In this study, we examined two different scenarios of compression and code rate:

i. R_{X1} = 0.833 and R_1= 0.75.
ii. R_{X1} = 0.75 and R_1= 0.80.

Figure 6 clearly depicts the energy consumptions per bit of the SISO, DSC-SISO and MIMO, DSC-MIMO as a function of distance for different compressing and code rates. The simulation result reveals that the energy consumption per bit of DSC-MIMO is less than that of the CMIMO, and the energy consumption per bit of the DSC-SISO is less than of the SISO at p = 1. The logic is that the DSC compresses the redundant source data and decreases the length of the data in the WSN. In Figure 6, the energy consumption per bit of SISO, DSC-SISO and MIMO, DSC-MIMO is represented as a function of distance for the compression rates, 83.3% and 75%, and it may be concluded that the energy consumption per bit is directly proportional to the compression rate

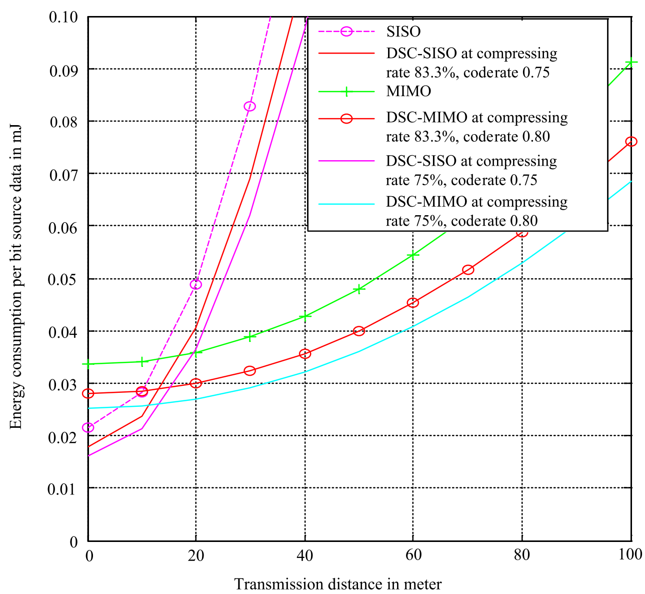

FIGURE 6 Energy consumption per bit for DSC-SISO, SISO, DSC-MIMO, and 2 × 2 MIMO at different compression and code rate for training overhead factor; p = 1

at training overhead factor $p = 1$. In Figure 6, the energy consumption per bit of SISO, DSC-SISO, MIMO, and DSC-MIMO for code rates, 0.75 and 0.80, is also depicted as a function of distance, and thus, it may be concluded that the energy consumption per bit is inversely proportional to the code rate at training overhead factor $p = 1$.

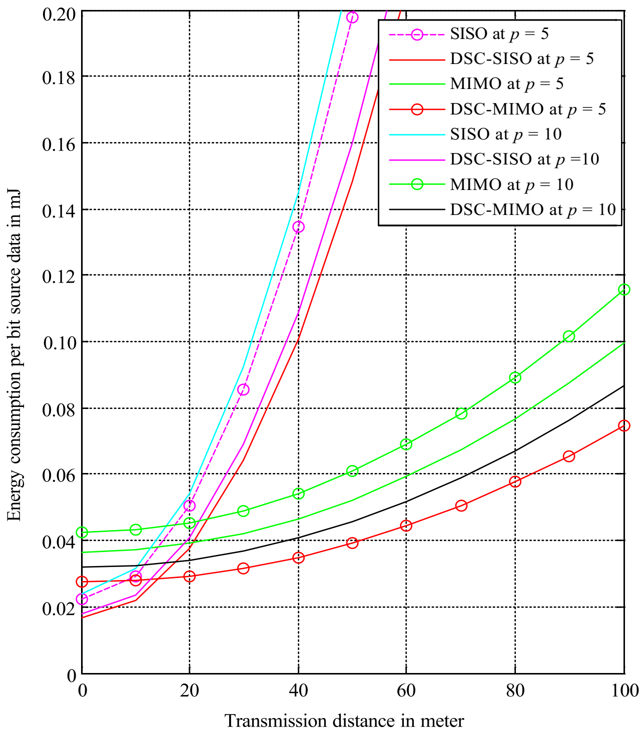

FIGURE 7 Energy consumption per bit of DSC-SISO, SISO, DSC-MIMO, and 2 × 2 MIMO against transmission distance at compression rate, 75%, code rate, 0.80, and training overhead factors, $p = 5$ and $p = 10$

TABLE 1 Simulation parameters

Symbol	Value
λ	0.125 m
A	0.47
$G_t G_r$	5 dBi
N_o	–174 dBm/Hz
B	10 KHz
P_{mix}	30.3 mW
P_{IFA}	2 mW
P_{syn}	50 mW
P_{filt}	2.5 mW
P_{filr}	2.5 mW
N_f	10 dB
P_{LNA}	20 mW
M_l	40 dB
P_{DAC}	15.43 mW
P_{ADC}	6.62 mW

The code rate is inversely proportional to the parity bits, in contrast to the message bits. Hence, the total consumption of energy is inversely proportional to the code rate. Figure 6 depicts that the MIMO scheme is very appropriate for long-distance communication, whereas the SISO is more suitable for short-distance communication. This is because, for long-range application, the transmission energy exceeds the circuit energy, and for short-range application, the circuit energy exceeds the transmission energy.

Figure 7 shows the energy consumption per bit of SISO, DSC-SISO, MIMO, and DSC-MIMO for the compression rate of 75% and code rate of 0.80 at $p = 5$ and $p = 10$. The simulation result shows that energy consumption per bit of the DSC-MIMO scheme is less than that of the CMIMO, and the energy consumption per bit of the DSC-SISO is less than that of the SISO at $p = 5$ and $p = 10$. The simulation result also shows that the energy consumption per bit is enhanced with increase in the training overhead factor (Table 1).

6 | ANALYTICAL APPROACH

Now, we concentrate on deriving a mathematical relation between p and v. We know that R_b^{eff} and R_b are related by the following relation [2]:

$$\begin{aligned} R_b^{eff} &= \frac{F - pN_T}{F} R_b \\ &= \frac{T_c R_s - pN_T}{T_c R_s} \\ &= \frac{\frac{3}{4f_m\sqrt{\pi}} R_s - pN_T}{\frac{3}{4f_m\sqrt{\pi}} R_s} R_b \\ &= \frac{\frac{3\lambda}{4v\sqrt{\pi}} R_s - pN_T}{\frac{3\lambda}{4v\sqrt{\pi}} R_s} R_b \end{aligned} \tag{28}$$

$$\text{or } \frac{R_b^{eff}}{R_b} = 1 - \frac{pN_T}{\frac{3\lambda}{4v\sqrt{\pi}} R_s},$$

$$\text{Velocity } (v) = \frac{3\lambda R_s}{4pN_T\sqrt{\pi}} \left(1 - \frac{R_b^{eff}}{R_b}\right). \tag{29}$$

The total energy consumption per bit when pN_T training symbols are introduced in every block is as follows:

$$\begin{aligned} E_{pbt} &= \frac{F}{(F - pN_T)} \left[\frac{P_{PA} + P_c}{R_b}\right], \\ E_{pbt} &= \frac{3\lambda R_S}{\left(3\lambda R_S - 4vpN_T\sqrt{\pi}\right)} \left[\frac{P_{PA} + P_c}{R_b}\right]. \end{aligned} \tag{30}$$

If the velocity is constant, then the block size (F) will remain constant for a specific value of carrier frequency. Therefore, the boundary value of p depends on $F - pN_T$ and the boundary condition is $p \le F/N_T$. The total consumption of energy becomes unideal, because the value of p does not fulfill the boundary condition. The same is true for changing the velocity, v, and making the training overhead fixed.

Figure 8 shows that the velocity increases proportionally with the symbol rate for a fixed value of p. For a fixed value of p, the rate of increase in velocity corresponding to the symbol rate reduces, the higher the number of transmitting nodes, as clearly depicted in the graph of velocity versus symbol rate. The simulation result shows that an increase in the symbol rate (R_s) increases the boundary values of the velocity while other parameters are constant.

Figure 9 shows that the velocity is inversely proportional to the training overhead factor for a constant symbol rate. For a fixed symbol rate, the rate of fall in velocity with the training overhead factor decreases with an increase in the number of the transmitting nodes.

In Figures 8 and 9, the simulation results also show that the MIMO technique reduces the boundary condition of training overhead factor or velocity while other parameters are kept fixed.

Figure 10 reveals that the total energy consumption of the DSC-MIMO and MIMO increases with velocity when the training overhead factor and other parameters are fixed. Figure 10 also shows that the energy consumption of the DSC-MIMO is less than that of the MIMO technique for a fixed velocity, distance, and training overhead factor because, in the DSC-MIMO, the DSC compresses the redundant source data and thus reduces the length of data in WSNs.

Figure 11 depicts the BER for code rates, 0.75, 0.80, and shows that the BER is directly proportional to the code rate. This is because, when the code rate increases, the message bit, compared to the parity increases.

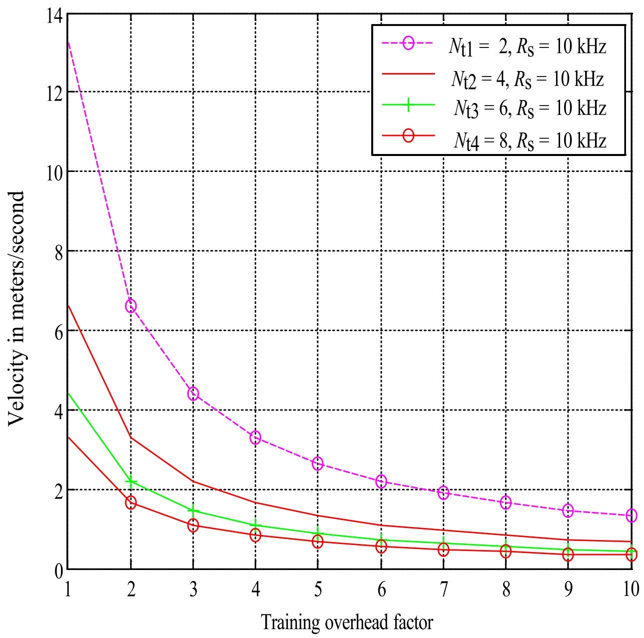

FIGURE 9 Velocity vs training overhead factor for fixed symbol rate

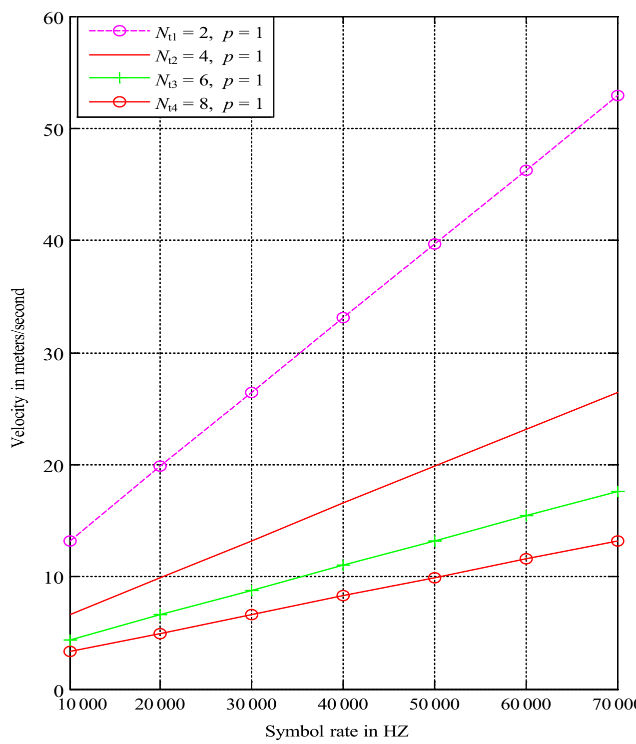

FIGURE 8 Velocity vs symbol rate for fixed training overhead factor

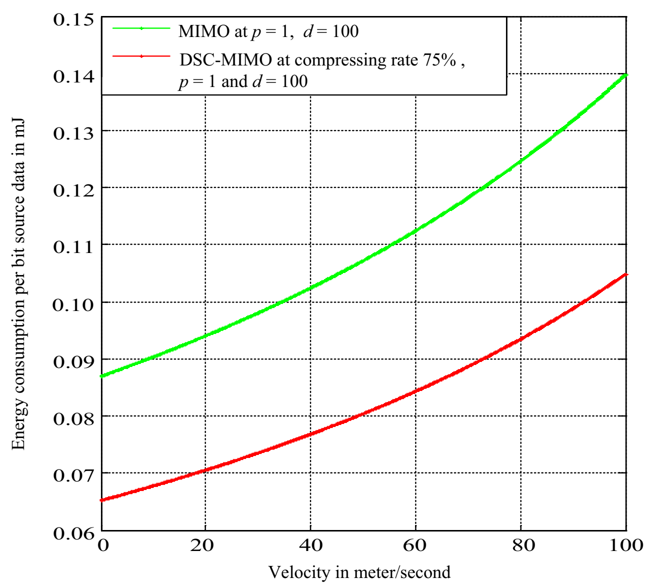

FIGURE 10 Energy consumption over velocity for fixed training overhead factor

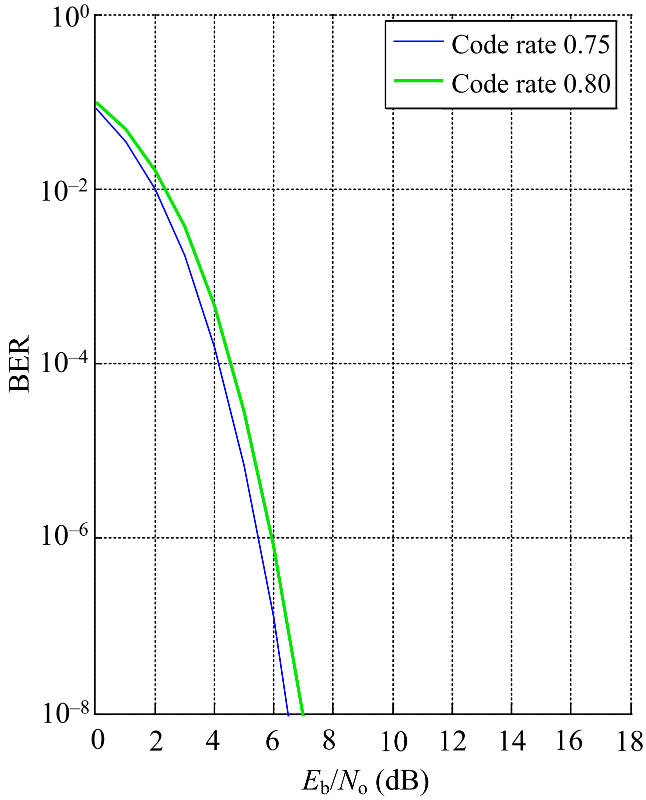

FIGURE 11 BER in additive white Gaussian noise (AWGN) channel block for code rate, 0.75 and 0.80, for BPSK modulation scheme

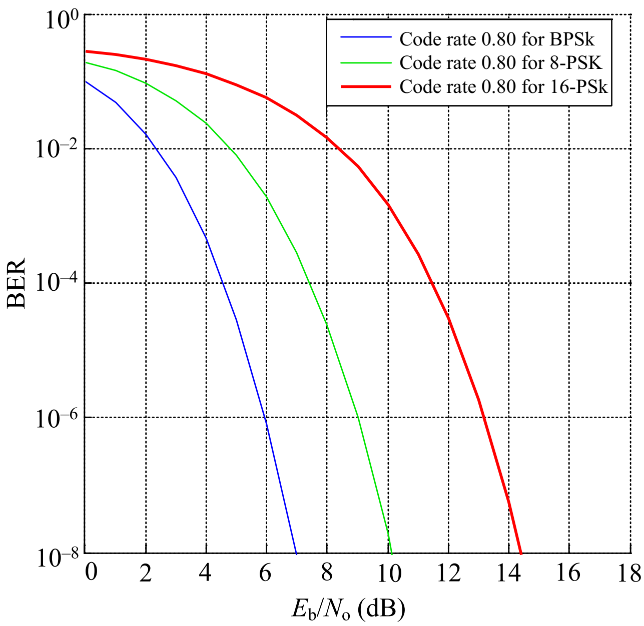

FIGURE 12 BER in AWGN channel block for code rate 0.80 and compression rate, 75% for different constellation sizes of phase-shift keying (PSK) modulation scheme

Figure 12 depicts the BER for BPSK, 8-PSK, and 16-PSK modulation techniques for code rate 0.80 in the AWGN channel. The simulation result shows that the BER is directly proportional to the constellation size. This is because the data rate is directly proportional to the bit per symbol for the same bandwidth, and therefore, the BER will also increase.

In Figure 13, the energy consumption by the CMIMO and DSC-MIMO for intercluster communication is depicted. The simulation result proves that the DSC-MIMO technique consumes less energy than that of the CMIMO when information from the same source is being sent in intercluster communication, because, in all the source nodes, the DSC compresses the correlated source data that lessens the energy consumption in the WSN.

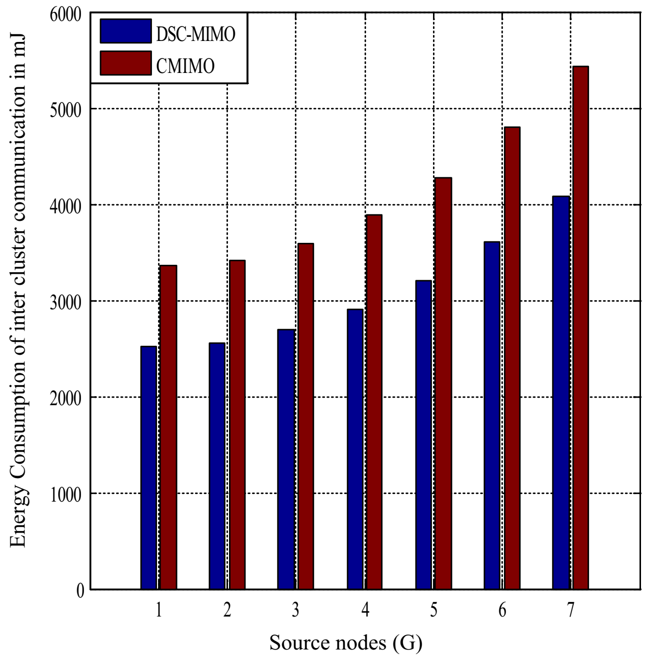

FIGURE 13 Energy consumption of CMIMO and DSC-MIMO for intercluster communication phase at compression rate, 75%

7 | CONCLUSION

The DSC-MIMO scheme has been utilized to compress redundant source data, and reduce the length of information, and thus, enhance the efficiency of the WSN. The simulation results demonstrate that the energy consumption of the DSC-SISO scheme is less, compared to the traditional SISO and the energy consumption that of the DSC-MIMO scheme is less than that of CMIMO. It also reveals that energy consumption reduces with an increase in the code rate and decrease in the compression rate in the WSN. The results reveal that energy consumption is directly proportional to the training overhead factor for fixed code and compression rates. It has also been shown that the energy consumption is enhanced by increment in the velocity and fixed training overhead factor. Thus, the DSC-MIMO is a significant method for reducing power consumption and improving the energy efficiency of the WSNs.

REFERENCES

1. S. Cui, A. J. Goldsmith, and A. Bahai, *Energy-efficiency of MIMO and cooperative MIMO techniques in sensor networks*, IEEE J. SAC **22** (2004), no. 6, 1089–1098.
2. S. K. Jayaweera, *Virtual MIMO-based cooperative communication for energy-constrained wireless sensor networks*, IEEE Trans. Wireless Commun. **5** (2006), no. 5, 984–989.
3. Z. Rafique, B.-C. Seet, and A. Al-Anbuky, *Performance analysis of cooperative virtual MIMO systems for wireless sensor networks*, IEEE Sens. **13** (2013), no. 6, 7033–7052.
4. Y. Peng et al., *Enhancing energy efficiency via cooperative MIMO in wireless sensor networks: state of the art and future research directions*, IEEE Commun. Mag. **55** (2017), 47–53.
5. M. Nasim, S. Qaisar, and S. Lee, *An energy efficient cooperative hierarchical MIMO clustering scheme for wireless sensor networks*, IEEE Sens. **12** (2012), 92–114.
6. N. Li, L. Zhang, and B. Li, *A new energy-efficient data transmission scheme based on DSC and virtual MIMO for wireless sensor network*, J. Contr. Sci. Eeng. **2015** (2015), 1–10.
7. H. Wang et al., *Cross-layer routing optimization in multirate wireless sensor networks for Distributed Source Coding based applications*, IEEE Trans. Wireless Commun. **7** (2008), no. 10, pp. 3999–4009.
8. S. K. Jayaweera et al., *Signal-processing-aided distributed compression in virtual MIMO-based wireless sensor networks*, IEEE Trans. Veh. Technol. **56** (2007), no. 5, 2630–2640.
9. N. Abughalieh et al., *A mutual algorithm for optimizing distributed source coding in wireless sensor networks*, Int. J. Distrib. Sens. Netw. **8** (2012), no. 2, 1–9.
10. S. A. Imam et al., *An energy-efficient data transmission scheme based on DSC-MIMO*, in Proc. IEEE Int. Conf. Integr. Circuits Microsyst. (Nanjing, China), Nov. 2017, pp. 309–312.
11. M. Sartipi and F. Fekri, *Distributed Source Coding in Wireless Sensor Networks using LDPC Coding: the Entire Slepian-Wolf Rate Region*, in Proc. IEEE Wireless Commun. Netw. Conf. (New Orleans, LA, USA), Mar. 2005, pp. 1939–1944.
12. M. Sartipi and F. Fekri, *Distributed source coding using short to moderate length rate-compatible LDPC codes the entire Slepian-Wolf rate region*, IEEE Trans. Commun. **56** (2008), no. 3, 400–411.
13. T. Sheltami, M. Musaddiq, and E. Shakshuki, *Data compression techniques in Wireless Sensor Networks*, Future Gener. Comp. Syst. **64** (2016), 151–162.
14. S. Haykin, *Digital Communication System*, Willy India Pvt. Ltd, New Delhi, India, 2015.
15. T. M. Cover and J. A. Thomos, *Elements of Information theory*, Wiley-Interscience publication, Hoboken, NJ, 2002.
16. M. Leinonen, M. Codreanu, and M. Juntti, *Distributed distortion-rate optimized compressed sensing in wireless sensor networks*, IEEE Trans. Commun. **66** (2018), no. 4, 1609–1623.
17. N. Deligiannis et al., *Distributed joint source-channel coding with copula-function-based correlation modeling for wireless sensors measuring temperature*, IEEE Sens. **15** (2015), 4496–4507.
18. J. Chen and X. Han, *The distributed source coding method research based on clustering wireless sensor networks*, Int. J. Sens. Netw. **17** (2015), no. 4, https://doi.org/10.1504/IJSNET.2015.069585.
19. M. Sartipi and F. Fekri. *Source and channel coding in wireless sensor networks using LDPC codes*, in Proc. Annu. IEEE Comuun. Soc. Conf. Sens. AD Hoc Commun. Netw. (Santa Clara, CA, USA), 2004, pp. 309–316.
20. M. R. Islam and Y. S. Han, *Cooperative MIMO communication at wireless sensor Network:An error correcting code approach*, Sens. **11** (2011), no. 10, 9887–9903.
21. T. S. Rappaport, *Wireless communications*, Prentice Hall of India, New Delhi, India, 2002.
22. S. Gravano, *Introduction of Error control*, Oxford University Press, Oxford, UK, 2001.

AUTHOR BIOGRAPHIES

Manish Kumar Singh received his BTech degree in Electronics and Communication Engineering from Uttar Pradesh Technical University, Lucknow, India in 2005 and his MTech degree in Communication Engineering from Shobhit University, Meerut, India in 2012. He is currently pursuing his PhD degree in Electronics and Communication Engineering from Jamia Millia Islamia University, New Delhi, India. Presently, he is an assistant professor at the Department of Electronics and Communication Engineering in KIET Group of Institutions, Ghaziabad, India. His research interests are Smart Sensors and Wireless sensor networks.

Syed Intekhab Amin received his Bachelor's degree in Electronics and Communication Engineering from The Institution of Engineers, India in 2006. He received his MTech degree in Electronic Circuits and System design from Zakir Hussain College of Engineering and Technology, Aligarh Muslim University, India, in 2009. He then obtained his PhD degree in 2017 from National Institute of Technology Jalandhar, India. He is presently an assistant professor in the department of Electronics and Communication Engineering, Jamia Millia Islamia, New Delhi, India. His research interests are wireless sensor networks, Device modeling for sensor application, Digital VLSI Circuits and System Design, Analog Circuits and System Design, and Reconfigurable FPGA implementations.